Published in final edited form as:
Acta Neuropathol. 2013 February ; 125(2): 215–229. doi:10.1007/s00401-012-1042-0.

Neurochemical mapping of the human hippocampus reveals perisynaptic matrix around functional synapses in Alzheimer's disease

Dávid Lendvai[#],
Department of Anatomy, Histology and Embryology, Semmelweis University, Budapest, Hungary

Markus Morawski[#],
Paul Flechsig Institute for Brain Research, Faculty of Medicine, Universita¨t Leipzig, Leipzig, Germany

László Négyessy,
Department of Theory, Wigner Research Centre for Physics, Institute for Particle and Nuclear Physics, Hungarian Academy of Sciences, Budapest, Hungary

Georgina Gáti,
Department of Anatomy, Histology and Embryology, Semmelweis University, Budapest, Hungary

Carsten Jäger,
Paul Flechsig Institute for Brain Research, Faculty of Medicine, Universita¨t Leipzig, Leipzig, Germany

Gábor Baksa,
Department of Anatomy, Histology and Embryology, Semmelweis University, Budapest, Hungary

Tibor Glasz,
Second Department of Pathology, Semmelweis University, Budapest, Hungary

Johannes Attems,
Institute for Ageing and Health, Newcastle University, Newcastle upon Tyne, UK

Heikki Tanila,
A.I. Virtanen Institute, University of Eastern Finland, Kuopio, Finland

Thomas Arendt,
Paul Flechsig Institute for Brain Research, Faculty of Medicine, Universität Leipzig, Leipzig, Germany

Tibor Harkany, and
European Neuroscience Institute, University of Aberdeen, Aberdeen AB25 2ZD, UK; Division of Molecular Neurobiology, Department of Medical Biochemistry and Biophysics, Karolinska Institutet, Stockholm, Sweden

Correspondence to: Thomas Arendt; Alán Alpár.
alan.alpar@ki.se; Thomas.Arendt@medizin.uni-leipzig.de.

Conflict of interest The authors declare that they have no conflict of interest.

Europe PMC Funders Author Manuscripts

Alán Alpár
Department of Anatomy, Histology and Embryology, Semmelweis University, Budapest, Hungary; European Neuroscience Institute, University of Aberdeen, Aberdeen AB25 2ZD, UK; Division of Molecular Neurobiology, Department of Medical Biochemistry and Biophysics, Karolinska Institutet, Stockholm, Sweden

[#] These authors contributed equally to this work.

Abstract

Perineuronal matrix is an extracellular protein scaffold to shape neuronal responsiveness and survival. Whilst perineuronal nets engulf the somatodendritic axis of neurons, axonal coats are focal extracellular protein aggregates surrounding individual synapses. Here, we addressed the chemical identity and subcellular localization of both perineuronal and perisynaptic matrices in the human hippocampus, whose neuronal circuitry is progressively compromised in Alzheimer's disease. We hypothesized that (1) the cellular expression sites of chondroitin sulphate proteoglycan-containing extracellular matrix associate with specific neuronal identities, reflecting network dynamics, and (2) the regional distribution and molecular composition of axonal coats must withstand Alzheimer's disease-related modifications to protect functional synapses. We show by epitope-specific antibodies that the perineuronal protomap of the human hippocampus is distinct from other mammals since pyramidal cells but not calretinin^{+} and calbindin^{+} interneurons, neurochemically classified as novel neuronal subtypes, lack perineuronal nets. We find that cartilage-related link protein 1 and brevican-containing matrices form isolated perisynaptic coats, engulfing both inhibitory and excitatory terminals in the dentate gyrus and entorhinal cortex. Ultrastructural analysis revealed that presynaptic neurons contribute components of perisynaptic coats via axonal transport. We demonstrate, by combining biochemical profiling and neuroanatomy in Alzheimer's patients and transgenic (APdE9) mice, the preserved turnover and distribution of axonal coats around functional synapses along dendrite segments containing hyperphosphorylated tau and in amyloid-β-laden hippocampal microdomains. We conclude that the presynapse-driven formation of axonal coats is a candidate mechanism to maintain synapse integrity under neurodegenerative conditions.

Keywords

Ageing; Ca^{2+}-binding protein; Human cortex; Interneuron; Neurodegeneration; Neuroprotection; Synaptic plasticity

Introduction

Neurons and glia are embedded in a highly organized extracellular matrix [21] whose chemical heterogeneity underpins many cellular processes, including axonal growth responses during neural development [32], the tuning of neuronal excitability [2, 64], and refining signalling at cell surface receptors [21, 27]. The intercellular matrix of the brain and spinal cord attracts clinically oriented research due to its putative effects on neuronal survival upon acute injury or chronic neurodegeneration [20, 23], and by promoting regeneration [24]. Extracellular matrix molecules fulfil their diverse roles by providing

individual scaffolds for neurons. Although this intercellular meshwork is largely amorphous, its condensed domains can surround the perisomatic compartment of certain subsets of neurons (“perineuronal nets”) [8, 31] or individual synapses (“axonal coats”) [11, 44, 53, 54].

Perineuronal nets are present in most vertebrates [8, 43, 46, 51, 59], including humans [1, 10, 11, 53, 54]. Their presence and distribution exhibit considerable regional variations, likely reflecting functional diversity of adult neuronal circuits [10, 30, 48, 55, 71]. As such, perineuronal nets can modulate the ionic milieu to maintain fast discharge behaviours in γ-aminobutyric acid-containing (GABAergic) interneurons [8, 30], protect neurons from stress [55, 71] and govern synaptic remodelling [4, 36, 64].

Modifications to the expression foci, composition and localization of perineuronal nets have been implicated in neuronal dysfunction in Alzheimer’s disease (AD), particularly by disrupting the pattern and timing of neuronal excitability [20, 23]. Experimental data [68], including genetic manipulations in mice [25, 39, 41, 42, 56, 58, 61], revealed cell type-specific requirements of extracellular matrix expression to promote neuronal survival. *Post-mortem* analysis of human neo- [10, 54, 55] or subcortical areas [53] revealed complementary distributions of histopathological AD hallmarks and chondroitin sulphate proteoglycans (CSPGs), suggesting the resistance of matrix-enwrapped neurons to AD-related pathologies. However, despite some biochemical data [62, 63], significant caveats exist in our knowledge regarding the extracellular matrix’s cell type specificity, structural complexity and molecular heterogeneity in the human hippocampus, the region most susceptible to neurodegeneration [60]. Particularly, it remains elusive whether perineuronal matrix surrounds spatially segregated synapse populations whose resistance to AD-related hippocampal pathology could rescue synaptic neurotransmission.

Here, we mapped perineuronal nets and axonal coats in the human hippocampal formation by combining light microscopy and ultrastructural analyses. CSPGs are particularly critical in the neural extracellular matrix since they form the molecular bridges between the cell surface and hyaluronan scaffolds [73]. Aggrecan and brevican are the main CSPG components, the former being an indispensable component of perineuronal nets [46, 73]. We show that the dentate gyrus (DG), Ammon’s horn subfields (CA1–CA4), subiculum and entorhinal cortex contain perineuronal nets and axonal coats with remarkable variations in their distribution patterns and neurochemical characteristics. Unexpectedly, perineuronal nets engulfed not only parvalbumin$^+$ but also calretinin$^+$ and calbindin$^+$ interneurons, highlighting key phylogenetic differences in the subclass diversity of hippocampal interneurons in comparison to other mammalian species [22]. Axonal coats selectively concentrated in the DG hilar region and entorhinal cortex, relied on the axonal transport of their components in presynaptic neurons, and surrounded a spatially defined yet neurochemically mixed synapse population. Through biochemical and morphological analyses of an AD patient cohort and transgenic model of amyloid β (Aβ) overexpression we show increased neuronal CSPG-based extracellular matrix expression in AD. The maintenance of axonal coats around vesicular neurotransmitter transporter-containing presynapses even if the subsynaptic dendrite contained hyperphosphorylated tau suggests

that axonal coats can provide a molecular scaffold to maintain synapse integrity in the diseased hippocampus.

Materials and methods

Tissues

Hippocampal tissues from severe and moderate AD patients and age-matched controls (n = 23 cases in total, both sexes, Table S1) [57], as well as from APPswe/PS1dE9 (APdE9) transgenic mice and littermate controls (n = 30 animals in total) were assigned to this study. Experimental protocols on human and mouse specimens were approved by local authorities and are available as Supplementary information (SI) online.

Immunohistochemistry and imaging

Chromogenic or multiple immunofluorescence histochemistry with select combinations of primary antibodies (Table S2) were according to published protocols [44, 57]. Sudan Black B counterstaining was used to quench tissue autofluorescence [65] (SI Materials and Methods). Results of chromogenic histochemistry were captured on either a Zeiss Axiovert 200 M microscope with a motorised stage (Märzhäuser, Germany), and using a CCD camera (Zeiss MRC) and MosaiX software connected to an Axiovision 4.6 image analysis system (Zeiss, Germany) or a Nikon Eclipse microscope. Sections processed for multiple immunofluorescence histochemistry were inspected and images acquired on a 710LSM confocal laser-scanning microscope (Zeiss). Procedural details of imaging are referred to in SI Materials and Methods.

Electron microscopy

Sections processed for aggrecan (HAG7D4 epitope) or brevican immunohistochemistry (chromogenic detection) were post-fixed in buffered 1 % OsO_4 at 22–24 °C for 1 h, and flat-embedded in Durcupan ACM (Fluka). The DG and CA regions were selected and embedded for ultrasectioning. Ultrathin sections (100 nm) were collected on single slot nickel grids coated with Formvar® and studied by using a Jeol 1200 EMX microscope (Tokyo, Japan). Primary magnifications ranged from 12,000× to 80,000×.

Western blotting

Protein samples prepared from human or mouse hippocampi were analysed under denaturing conditions. Western blot analysis was undertaken as described [57] with primary antibodies listed in Table S2. Blots were scanned using a Bio-Rad XRS^+ imaging platform and quantified with Image Lab 3.01 (Bio-Rad Laboratories). CSPG concentrations were normalized to β-actin (1:10,000; Sigma) used as loading control throughout.

Statistical analysis

Data were analysed using Statistical Package for the Social Sciences (version 17.0, SPSS Inc.). Integrated optical densities of the immunoreactive targets in Western blotting experiments were evaluated using Student's t test (on independent samples). Data were expressed as mean ± SEM. A p value of <0.05 was considered statistically significant.

Results

General considerations

We performed high resolution and correlated bright field, confocal laser-scanning and electron microscopy to reveal the chemical heterogeneity and compartmentalization of the CSPG-based extracellular matrix in the human hippocampal formation and entorhinal cortex by antibodies directed against non-overlapping molecular domains of aggrecan, brevican and CRTL-1 (Figs. 1a, b–b_2, 2a–a_2, 3a–a_2, 4a–a_2, S2a). Key inferences of our analysis include phylogenetic differences in the laminar distribution, subcellular recruitment [perineuronal nets, dendritic sheaths (Fig. 1c–e_3) and axonal coats], and the molecular identity of neuronal subtypes expressing CSPG-based perineuronal matrix. However, *Wisteria floribunda* agglutinin (WFA; Fig. 1f_3), which is rapidly degraded during *post-mortem* delay [54] (and SI Materials and Methods), only sparsely identified hippocampal neurons with case-to-case variability in its distribution. This notion led us to test whether aggrecan$^+$ matrix assemblies were under-sampled or their phenotypes had changed due to epitope masking in our post-mortem tissues (Fig. 1f–f_3'). By performing chondroitinase digestion of chondroitin sulphate side-chains (Fig. 1a), and using perfusion-fixed mouse tissues as positive controls (Fig. 1g, g′), we confirmed that neither the distribution pattern nor the intensity/phenotype of aggrecan-containing perineuronal nets (as per antibody recognition, sensitivity and detectability) were affected in the *post-mortem* human hippocampus.

Aggrecan in the human hippocampal formation

Aggrecan is an indispensable component of the brain's extracellular matrix (Fig. 1a), particularly perineuronal nets [15, 28, 46]. Although the analysis of aggrecan functions in the adult brain is curtailed by the failure of aggrecan knock-out mice to survive into adulthood [69], this protein is critical for the initial [69] activity-dependent assembly of perineuronal nets [50], and is retained throughout life as a major matrix component [73]. By using antibodies directed against aggrecan's CSPG-enriched (AB1031 and Cat-301) or N-terminal (HAG7D4) domains (Fig. 1a), we have studied the distribution and compartmentalization of this CSPG component in the human hippocampal formation, including the entorhinal cortex.

We detected perineuronal nets in all hippocampal subfields in a region- and layer-specific manner (Fig. 2a–a_2, Fig. S2a). The distribution of AB1031-positive(+), Cat-301$^+$ or HAG7D4$^+$ perineuronal nets was overlapping, failed to label pyramidal cells (Fig. 2a_2), yet differed in their intensity to label the hippocampal neuropil (Fig. 2a, a_1, Fig. S2a). Perineuronal nets were most frequently seen in the CA1 region (Fig. 2a–f), particularly in stratum oriens surrounding multipolar non-pyramidal neurons (Fig. 2a–a_2, b, d, f). Whilst the pyramidal layer was largely devoid of aggrecan$^+$ somata, many perineuronal nets of multi- or bipolar phenotypes were identified in strata radiatum and lacunosum-moleculare (Fig. 2c, e, Fig. S1-3). The entorhinal cortex could typically be demarcated via the intense labelling of its principal strata (Fig. 2a–a_2, Fig. S2a) [6]. We refer to the Supplementary information (Fig. S1-3) for detailed description of the distribution and morphology of aggrecan$^+$ perineuronal matrix.

Perineuronal nets were of different phenotypes, including sharply contoured “classical” or “diffuse” subtypes [70]. This diversity was best reflected by the appearance of AB1031$^+$ perineuronal nets throughout the human hippocampus (Fig. 2b, c). AB1031$^+$, Cat-301$^+$ or HAG7D4$^+$ matrix assemblies formed dendritic sheaths that extended for >50 μm over second to third order dendrites (Fig. 2b–f). Putative axon initial segments were identified as thin structures emanating from the soma or the most proximal part of a first order dendrite (Fig. 2b, b_1) [13]. At the ultrastructural level, aggrecan typically enwrapped postsynaptic compartments on dendrites and dendritic spines (Fig. 2g–i). This aggrecan-containing matrix assembly was often seen over axon terminals and presynaptic axons, encapsulating the entire synapse (Fig. 2g–i).

CRTL-1 is recruited to axonal coats at excitatory and inhibitory synapses

The core assembly of brain extracellular matrix is established by “link” proteins, which connect CSPGs to hyaluronan (Fig. 1a) [52, 73]. The CRTL-1 protein is an indispensable component of perineuronal nets, its production being the major event to limit synaptic plasticity via organizing CSPGs into perineuronal nets [14, 15]. Animals lacking CRTL-1 have disrupted perineuronal nets and persistent synaptic plasticity [14].

CRTL-1$^+$ perineuronal nets and *axonal coats* exhibited layer- and region-specific distribution in the profusely stained neuropil (Fig. 3a–a_3). Compared to our aggrecan “maps” (Fig. S4), CRTL-1$^+$ perineuronal nets in the CA1 subfield were less densely packed, and restricted to strata oriens and radiatum. These were of the sharply contoured “conventional” type of perineuronal nets with extensive peridendritic sheaths (Fig. 3b, b_1). In the CA2 subfield (Fig. 3a, a_1), perineuronal nets were seen in the strata oriens and radiatum (Fig. 3e). Notably, distinct neuropil labelling in the CA2 subfield formed a “barrier” separating the CA1 and CA3 regions (Fig. 3a). This finding is supported by earlier data from rodents, reporting dense extracellular matrix proteoglycan and lectin reactivity of the neuropil in the corresponding subfield [9, 12]. In contrast to our anti-aggrecan immunostainings, perineuronal nets were frequently encountered in all layers of the CA3 region with the putative axon initial segment occasionally visible (Fig. 3c). Alternatively, the perineuronal matrix assembly was restricted to the somata as faint CRTL-1$^+$ perisomatic rims (Fig. 3d). In subicular regions and the entorhinal cortex, perineuronal nets surrounded multipolar neurons (Fig. $3a_3$). The entorhinal cortex was decorated by prominently labelled islands in the external principal stratum [6] (Fig. 3f).

The dentate hilus contained many perineuronal nets (Fig. 3a). However, we have encountered a large number of densely packed structures of 1–3 μm in diameter, *axonal coats* [11], at the hilar border of the granular layer (Fig. 3g, g_1). Axonal coats were identified in a similarly high density in the entorhinal cortex; significantly exceeding those in the CA regions ($p < 0.05$; Fig. $3g_1$). Ultrastructural analysis showed that, in addition to the presence of CRTL-1 in myelinated axons (Fig. 3h, i), extracellular CRTL-1$^+$ matrix is restricted to surround terminal axon segments including the synapse (Fig. 3j, k).

We used high-resolution confocal microscopy to show that perineuronal nets engulfed excitatory and inhibitory perisomatic synapses immunoreactive for vesicular glutamate transporter 1 (VGLUT1) and glutamic acid decarboxylase 65/67 isoforms (GAD65/67),

respectively (Fig. 3l–m_1). Notably, dendrite-targeting "distal" synapses were also embedded in aggrecan/CRTL-1^+ peridendritic sheaths (Fig. 5n, n_1). Next, we asked if synapses can develop axonal coats in the absence of perisomatic or peridendritic matrices. We found single presynaptic sites surrounded by CRTL-1+ axonal coats in the hilar region of the dentate gyrus (Fig. 3o).

Brevican (50 kDa fragment) accumulates in axonal coats

Brevican is a brain-specific proteoglycan primarily produced by glia [34, 72]. Brevican's roles in synapse development and signalling were shown during the formation of cerebellar glomeruli [72] and by disrupted hippocampal long-term potentiation in brevican-deficient mice [7]. Brevican is proteolytically cleaved into N-terminal (50 kDa) and intermediate/C-terminal (90 kDa) fragments [45]. Here, we used an antibody raised against Brevican's 50 kDa fragment (gift of Dr. R. Matthews) to show that the brevican$^+$ extracellular matrix pattern of the human hippocampal formation is remarkably different from other matrix maps hitherto identified (Fig. 4a–a_3).

Perineuronal nets (Fig. 4b–c) were sporadically found in the strata oriens and radiatum of the CA1–CA4 subfields. Instead, brevican predominantly identified axonal coats, arranged as pearl lace-like strings, at the hilar surface of the dentate granule layer (Fig. 4d–d_3). The orientation of axonal ribbons resembled the aggrecan$^+$ peridendritic sheaths at the hilar margin of the granule layer (Fig. S1g). Although at markedly lower densities, axonal coats were also seen in the CA1–CA3 subfields (except the stratum cortex, brevican$^+$ axonal coats re-appeared at a high density ($p < 0.05$ vs. CA subfield; Fig. $4d_3$).

We used ultrastructural analysis to confirm that brevican$^+$ axonal coats surrounded synapses. We show that brevican$^+$ matrix assemblies were restricted to individual synapses without forming extensive intercellular scaffolds along the postsynaptic dendrites or somata (Fig. 4e–g). Electron microscopy demonstrated the presence of brevican immunoreactivity in myelinated axons (Fig. 4h, i). This finding, and the lack of brevican immunoreactivity in endo- or lysosomes (*data not shown*), suggest that presynaptic neurons actively shape axonal coats.

Perineuronal nets surround parvalbumin$^+$, calretinin$^+$ and calbindin$^+$ hippocampal neurons

Confirming earlier observations in other mammalian species or areas of the human nervous system [17, 29], the majority of parvalbumin$^+$ cells were surrounded by aggrecan-containing perineuronal nets (Fig. $5a_1$–c_1). The association of CRTL-1^+ perineuronal nets and parvalbumin$^+$ cells was analogously high; with CRTL-1^+ extracellular matrix frequently surrounding neurons in stratum oriens (Fig. 5d) but not stratum radiatum (Fig. 5e).

Calretinin$^+$ and calbindin D28k$^+$ neurons of lower mammals lack perineuronal nets [17, 22]. In contrast, a subpopulation of calretinin$^+$ neurons was surrounded by aggrecan$^+$ (Fig. 5f, f_1) or CRTL-1^+ (Fig. 5g) perineuronal nets in the human hippocampus. Similarly, calbindin D28k$^+$ neurons were—though less frequently—surrounded by aggrecan$^+$ perineuronal nets (Fig. 5a). Overall, while the presence of perineuronal nets is a general hallmark of inhibitory neurotransmission (Fig. 5h), our data suggest that the human hippocampus contains a unique variety of perineuronal net-bearing interneurons.

Perisynaptic matrix assemblies are spared in the hippocampus in Alzheimer's disease

Impaired hippocampal synaptic neurotransmission is recognized as a key event underpinning AD-related cognitive impairment. Perineuronal nets and axonal coats have been implicated in maintaining microenvironmental conditions supporting synaptic neurotransmission [8, 54]. Yet modifications to the composition or regional distribution of axonal coats in the human hippocampus during progression of AD, in particular their relationship to cytoskeletal abnormalities, remain elusive. Therefore, we asked whether expression levels of extracellular matrix CSPG components change in the AD hippocampus. By Western blotting of protein lysates (Fig. 6a) from clinico-pathologically verified subjects [57] and age-matched controls (Table S1) we found transiently, albeit non-significantly, reduced brevican, CRTL-1, and aggrecan (AB1031) levels when comparing control versus "moderate" AD subjects (Fig. 6b–b_3). In contrast, "definite/severe" AD cases showed significantly increased ($p < 0.05$) brevican and CRTL-1 levels relative to age-matched controls (Fig. 6b–b_3).

Next, we have addressed AD-related structural arrangements by localizing CRTL-1^+ axonal coats in the proximity of Aβ plaques and along granule cell dendrites with (and without) neurofibrillary pathology (hyperphosphorylated tau), the primary pathological hallmarks of AD. We found that axonal coats morphologically and neurochemically indistinguishable from those in age-matched control brains (Fig. 6c) were retained in the proximity of Aβ plaques in "definite" AD (Fig. 6d–d_2). Notably, axonal coats were found distributed along dendrite segments containing hyperphosphorylated tau (Fig. 6e–e_2) at densities identical to those seen along dendrites without tau pathology (Fig. 6f–g) and identified by microtubule-associated protein 2 immunoreactivity (Fig. 6f_2). We have extended these findings by showing that perineuronal nets exhibited mutually exclusive distribution with hyperphosphorylated tau in the DG hilus (Fig. 6h, S5a-a_2).

Axonal coats around VGAT$^+$ and VGLUT1$^+$ synapses in transgenic mice with AD-like pathology

Axonal coats around Aβ plaques and apposing hyperphosphorylated tau-containing dendrites may suggest the stability of select synapse populations. The alternative hypothesis may be that axonal coat stability is uncoupled from synapse integrity and CRTL-1^+ axonal coats are in fact remnants of extracellular scaffolds at degenerating synaptic sites. We have addressed this hypothesis in APdE9 mice at successive ages characterized by robust hippocampal Aβ plaque burden [33] by biochemical CPSG matrix profiling and high-resolution microscopy. Seven and 10-month-old APdE9 mice exhibited moderate yet opposite shifts in hippocampal brevican (Fig. 7a, b, S6a,b) and CRTL-1 (Fig. 7a, b_1, S6a,b_1) levels. In contrast, the concentration of aggrecan's 450 kDa isoform progressively and significantly increased ($p < 0.05$ vs. wild-type littermates at 10 months; Fig. 7a, b_2, S6a, b_2). We found a positive relationship between brevican and VGLUT1 levels in wild-type mice (brevican: $R^2 = 0.71$, $p < 0.05$; Fig. S6c),which was lost in APdE9 transgenics (Fig. S6c-c_2). However, the positive relationship of brevican and vesicular GABA transporter was maintained (VGAT; $R^2 = 0.69$, $p < 0.05$; Fig. S6d), yet at considerably lower levels in APdE9 mice ($R^2 = 0.67$, $p < 0.05$; Fig. S6d-d_2). Although the APdE9 model may be limited to recapitulate the full extent of human pathomechanisms, it is remarkable to note the

analogous change in CSPG expression under worsening conditions in mice and human subjects.

Next, we have addressed the distribution and neurochemical identity of axonal coat-bearing synapses. We found axonal coats at high densities in the vicinity of or occasionally in direct contact with Aβ plaques (Fig. 7c, c_1, S6e,f). Next, we hypothesized that axonal coats surround functional synapses. We have addressed this possibility by the combined detection of VGAT/CRTL-1 and VGLUT1/brevican since VGAT and VGLUT1 are indispensable to shuttle the respective neurotransmitters into presynaptic vesicles [49]. We showed that CRTL-1^+ axonal coats surrounded $VGAT^+$ synaptic profiles in the immediate vicinity of Aβ deposits (Fig. 7d–d_3, Fig. S5b-b″). Similarly, $brevican^+$ axonal coats surrounded excitatory $VGLUT1^+$ terminals (Fig. 7e–e_2, S5c-c_1″). These data suggest that axonal coats engulf synapses that had retained their ability of neurotransmitter release under conditions of Aβ pathology.

Discussion

Extracellular matrix patterning in the human hippocampus

Learning and memory processing in the hippocampus require a unique capacity of activity-driven synapse dynamics and reorganization throughout life. Yet retained neuroplasticity renders hippocampal neurons exceedingly vulnerable to ageing or stress [47]. Perineuronal nets might contribute to both synapse formation and signalling: focal accumulation of the extracellular matrix can stabilize new synaptic contacts [4, 64]. Once mature, perineuronal nets can attenuate stochastic ionic imbalances to protect neurons from excitotoxicity, oxidative stress or Aβ accumulation during ageing and in AD [10, 54, 55]. Therefore, the relatively low density of perineuronal nets in the human hippocampus, particularly in comparison to primary neocortical areas [10], may not only allow the high turnover of excitatory and/or inhibitory synapses associated with information flow but also reveal a “site of vulnerability” in the human hippocampus.

We performed the comparative analysis of CSPG matrix components in the human hippocampus at the cellular and subcellular levels (Fig. S4). Phylogenetic differences include: (1) the lack of perineuronal nets around hippocampal principal cells [66]. Although at low numbers, net-bearing pyramidal cells are regularly observed in lower mammals [10]. (2) The presence of perineuronal nets around $calretinin^+$ and $calbindin^+$ interneurons, in addition to $parvalbumin^+$ basket cells [17, 22], suggests novel molecular modalities amongst hippocampal interneuron subtypes in humans. (3) The unexpectedly high density of axonal coats, a recently described form of the extracellular matrix around individual synapses [11], in the hilar region of the dentate gyrus and the entorhinal cortex, the most vulnerable and plastic loci of the hippocampal formation [40] with the latter showing the first signs of neurofibrillary tangle formation in AD [19]. (4) The invariable presence of axonal coats in the proximity of senile plaques and apposing hyperphosphorylated tau-containing dendrites. Increased brevican and CRTL-1 levels in AD might either reflect ectopic axonal sprouting around senile plaques or suggest a shift in extracellular matrix synthesis or utilization. The regional and subcellular distribution and presynaptic axonal transport of CRTL-1 and brevican suggest that these proteins might be enriched, irrespective of their neuronal or glial

origins, in the same synapse population (Fig. 6d). (5) Axonal coats surround synapses whose vesicular neurotransmitter transporter content suggests synaptic neurotransmission even in the presence of experimentally high Aβ in APdE9 mice.

Parvalbumin$^+$ interneurons: a conserved family with a novel human hippocampal subtype

Parvalbumin expression characterizes basket and chandelier cells [26, 37]. Irrespective of their presence in all regions of the mammalian hippocampus [5], perineuronal nets invariably and selectively surround parvalbumin$^+$ interneurons [16, 29]. In the human hippocampus, we find that CRTL-1-containing perineuronal nets only enwrapped parvalbumin$^+$ interneurons in the stratum oriens but not radiatum. The selective absence of CRTL-1$^+$ perineuronal nets around parvalbumin$^+$ somata in stratum radiatum may suggest the existence of a novel subtype of parvalbumin$^+$ interneurons in the human brain. However, (1) parvalbumin$^+$ interneurons are of relatively low abundance in stratum radiatum [26], (2) not all parvalbumin$^+$ cells are surrounded by perineuronal nets (Fig. 7b, b_1) [29] and (3) parvalbumin$^+$ cells are heterogeneous in their HAG7D4 immunoreactivities. Thus, the chemical heterogeneity of the extracellular matrix even within a single subclass of interneurons may allude to a relationship between the formation of perineuronal nets and the recruitment of particular interneurons to functionally defined hippocampal neuronal networks.

Perineuronal nets surround calretinin$^+$ and calbindin$^+$ interneurons

Calretinin$^+$ interneurons are devoid of perineuronal nets in the mammalian species studied so far [17, 22]. In contrast, and although at significantly lower densities than their parvalbumin$^+$ counterparts, calretinin$^+$ interneurons were enveloped by CSPG-containing perineuronal nets in the human hippocampus. Due to their smooth dendrites and positioning outside the mossy fibres region, we propose that perineuronal net-bearing calretinin$^+$ cells are interneurons “specialized to innervate other interneurons” [26]. Perineuronal net-bearing calretinin$^+$ neurons may be specific for the human hippocampus since similar cellular arrangements have not been reported earlier.

Perisynaptic coats preferentially localize to the hilus in the human hippocampus

Perineuronal nets have apertures at points of synaptic contacts [17]. This assembly gives mechanical and chemical support to stabilize the synapse [27, 64]. In the human hippocampus, we find that both excitatory and inhibitory synapses may be engulfed by perisomatic extracellular matrix produced by the postsynaptic cell. Nevertheless, synapses embedded in perineuronal nets are only a fraction of all synaptic contacts. Instead, individual matrix “rings”, termed axonal coats, can encapsulate synapses. Axonal coats are also present in the basal ganglia [11] and thalamus [44] of humans, particularly around inhibitory nerve terminals. Here, we find that CRTL-1$^+$ or brevican$^+$ axonal coats enwrap non-perisomatic synapses in the hippocampus. CRTL-1$^+$ axonal coats around excitatory pre-terminals were typically identified in the hilar region of dentate gyrus and neighbouring CA3 stratum radiatum. The focal concentration of matrix-laden boutons suggests that these may belong to mossy fibre collaterals. Postsynaptic neurons are generally viewed as the source of the perisynaptic matrix, particularly when perisomatic (inhibitory) synapses are embedded in the matrix assembly of perineuronal nets [17]. Our findings at the

Europe PMC Funders Author Manuscripts

ultrastructural level, however, suggest that axonal coat constituents can undergo anterograde axonal transport, suggesting their presynaptic origin.

Expression of CSPG proteins in Alzheimer's disease

It is increasingly appreciated that AD-related cognitive decline is due to the impairment of synaptic integrity [18]. Perineuronal nets and axonal coats can shape the "micromilieu" of individual neurons. Therefore, any change in the molecular heterogeneity of the extracellular matrix may trigger neuronal dysfunction. Initial insights in AD-related changes to chondroitin sulphates suggested their dramatic increase [67]. In contrast, lectin levels (e.g. WFA) reportedly decrease in AD [3, 38]. However, lectin reactivity progressively decreases as a factor of *post-mortem* delay [54], asking a re-visit of earlier data. More recently, the composition and assembly of the CSPG-based extracellular matrix in iso- or subcortical areas were shown to remain unaltered in both transgenic models of AD [56] and human autopsy material [35, 53, 54]. Since the archicortex (e.g., entorhinal cortex and hippocampus) is particularly sensitive to ageing and neurodegeneration [47], we hypothesized that aggrecan and/or brevican expression may be affected in AD.

It is broadly accepted, and confirmed here, that perineuronal net-bearing neurons are spared from AD-related cytoskeletal pathology [10]. This notion is underscored by the vulnerability of subcortical neurons (e.g., nucleus basalis of Meynert, raphe nuclei or locus ceruleus), which only infrequently express perineuronal nets [53]. This report identifies a separate subcellular niche in which CSPGs accumulate. We recognize the presynaptic neuron as a likely source contributing CSPGs to axonal coats, thus preserving the structural integrity of the presynapse, and probably uncoupling it from postsynaptic (dendritic) cytoskeletal pathologies.

We found that axonal coats are structurally stable subcellular specializations during AD progression in the hippocampus. The existence of perisynaptic matrix assemblies around senile plaques or apposing hyperphosphorylated tau-containing dendrite segments does not merely reflect retained yet non-functional scaffolds. Instead, axonal coats enwrap synapses endowed with vesicular neurotransmitter transporters, which was further underpinned by the persisting positive correlation between brevican and vesicular GABA transporter concentrations. Increases in both brevican and CRTL-1 levels corroborate our morphological findings, reflecting increased turnover and utilization of extracellular matrix components to preserve synapse integrity, a neuronal response to injury. Alternative processes may include ectopic axonal sprouting—irrespective of the terminals' ability to reach functionality—around senile plaques (Fig. 7 and S6) or preferred survival of axonal coat-bearing synapses, which may result in synaptic imbalance, compromising the functional efficacy of the global hippocampal network in AD. Thus, axonal coats represent a novel, spatially organized and neurochemically defined molecular feature of the hippocampal circuitry whose manipulation might not only protect the structural integrity of synapses but also facilitate information "flow" underpinning cognition [21].

Supplementary Material

Refer to Web version on PubMed Central for supplementary material.

Acknowledgments

The authors thank G. Brückner and R. Matthews for comments and antibodies, and T. Hortobágyi (London Neurodegenerative Diseases Brain Bank, United Kingdom) for *post-mortem* human hippocampal tissues used in biochemical assays. This work was supported by the Scottish Universities Life Science Alliance (T.H., A.A.), the German Research Foundation GRK 1097 “INTERNEURO” (T.A.; M.M), the EU-Project “Neuropro” (Grant Agreement No. 223077), the COST Action BM1001 “Brain Extracellular Matrix in Health and Disease”, the Alzheimer Forschungsinitiative e.V. (AFI#11861, M.M.), the Dunhill Medical Trust (R173/1110; J.A.), the Swedish Research Council (T.H.) and the European Union FP7 MEMOLOAD grant (HEALTH-F2-2007-201159, H.T. and T.H.).

References

1. Adams I, Brauer K, Arelin C, Hartig W, Fine A, Mader M, Arendt T, Bruckner G. Perineuronal nets in the rhesus monkey and human basal forebrain including basal ganglia. Neuroscience. 2001; 108:285–298. [PubMed: 11734361]
2. Amet LE, Lauri SE, Hienola A, Croll SD, Lu Y, Levorse JM, Prabhakaran B, Taira T, Rauvala H, Vogt TF. Enhanced hippocampal long-term potentiation in mice lacking heparin-binding growth-associated molecule. Mol Cell Neurosci. 2001; 17:1014–1024. [PubMed: 11414790]
3. Baig S, Wilcock GK, Love S. Loss of perineuronal net N-acetylgalactosamine in Alzheimer’s disease. Acta Neuropathol. 2005; 110:393–401. [PubMed: 16133543]
4. Berardi N, Pizzorusso T, Ratto GM, Maffei L. Molecular basis of plasticity in the visual cortex. Trends Neurosci. 2003; 26:369–378. [PubMed: 12850433]
5. Bertolotto A, Rocca G, Canavese G, Migheli A, Schiffer D. Chondroitin sulfate proteoglycan surrounds a subset of human and rat CNS neurons. J Neurosci Res. 1991; 29:225–234. [PubMed: 1890701]
6. Braak H, Braak E. The human entorhinal cortex: normal morphology and lamina-specific pathology in various diseases. Neurosci Res. 1992; 15:6–31. [PubMed: 1336586]
7. Brakebusch C, Seidenbecher CI, Asztely F, Rauch U, Matthies H, Meyer H, Krug M, Bockers TM, Zhou X, Kreutz MR, Montag D, et al. Brevican-deficient mice display impaired hippocampal CA1 long-term potentiation but show no obvious deficits in learning and memory. Mol Cell Biol. 2002; 22:7417–7427. [PubMed: 12370289]
8. Bruckner G, Brauer K, Hartig W, Wolff JR, Rickmann MJ, Derouiche A, Delpech B, Girard N, Oertel WH, Reichenbach A. Perineuronal nets provide a polyanionic, glia-associated form of microenvironment around certain neurons in many parts of the rat brain. Glia. 1993; 8:183–200. [PubMed: 7693589]
9. Bruckner G, Grosche J, Hartlage-Rubsamen M, Schmidt S, Schachner M. Region and lamina-specific distribution of extracellular matrix proteoglycans, hyaluronan and tenascin-R in the mouse hippocampal formation. J Chem Neuroanat. 2003; 26:37–50. [PubMed: 12954529]
10. Bruckner G, Hausen D, Hartig W, Drlicek M, Arendt T, Brauer K. Cortical areas abundant in extracellular matrix chondroitin sulphate proteoglycans are less affected by cytoskeletal changes in Alzheimer’s disease. Neuroscience. 1999; 92:791–805. [PubMed: 10426522]
11. Bruckner G, Morawski M, Arendt T. Aggrecan-based extracellular matrix is an integral part of the human basal ganglia circuit. Neuroscience. 2008; 151:489–504. [PubMed: 18055126]
12. Bruckner G, Seeger G, Brauer K, Hartig W, Kacza J, Bigl V. Cortical areas are revealed by distribution patterns of proteoglycan components and parvalbumin in the Mongolian gerbil and rat. Brain Res. 1994; 658:67–86. [PubMed: 7834357]
13. Bruckner G, Szeoke S, Pavlica S, Grosche J, Kacza J. Axon initial segment ensheathed by extracellular matrix in perineuronal nets. Neuroscience. 2006; 138:365–375. [PubMed: 16427210]
14. Carulli D, Pizzorusso T, Kwok JC, Putignano E, Poli A, Forostyak S, Andrews MR, Deepa SS, Glant TT, Fawcett JW. Animals lacking link protein have attenuated perineuronal nets and persistent plasticity. Brain. 2010; 133:2331–2347. [PubMed: 20566484]
15. Carulli D, Rhodes KE, Fawcett JW. Upregulation of aggrecan, link protein 1, and hyaluronan synthases during formation of perineuronal nets in the rat cerebellum. J Comp Neurol. 2007; 501:83–94. [PubMed: 17206619]

16. Celio MR. Perineuronal nets of extracellular matrix around parvalbumin-containing neurons of the hippocampus. Hippocampus. 1993
17. Celio MR, Spreafico R, De BS, Vitellaro-Zuccarello L. Perineuronal nets: past and present. Trends Neurosci. 1998; 21:510–515. [PubMed: 9881847]
18. Crews L, Masliah E. Molecular mechanisms of neurodegeneration in Alzheimer's disease. Hum Mol Genet. 2010; 19:R12–R20. [PubMed: 20413653]
19. de CA, Polydoro M, Suarez-Calvet M, William C, Adamowicz DH, Kopeikina KJ, Pitstick R, Sahara N, Ashe KH, Carlson GA, Spires-Jones TL, et al. Propagation of tau pathology in a model of early Alzheimer's disease. Neuron. 2012; 73:685–697. [PubMed: 22365544]
20. Dityatev A, Fellin T. Extracellular matrix in plasticity and epileptogenesis. Neuron Glia Biol. 2008; 4:235–247. [PubMed: 19497143]
21. Dityatev A, Seidenbecher CI, Schachner M. Compartmentalization from the outside: the extracellular matrix and functional microdomains in the brain. Trends Neurosci. 2010; 33:503–512. [PubMed: 20832873]
22. Drake CT, Mulligan KA, Wimpey TL, Hendrickson A, Chavkin C. Characterization of *Vicia villosa* agglutinin-labeled GABAergic interneurons in the hippocampal formation and in acutely dissociated hippocampus. Brain Res. 1991; 554:176–185. [PubMed: 1933299]
23. Ferhat L, Chevassus-Au-Louis N, Khrestchatisky M, Ben-Ari Y, Represa A. Seizures induce tenascin-C mRNA expression in neurons. J Neurocytol. 1996; 25:535–546. [PubMed: 8910799]
24. Fitch MT, Silver J. CNS injury, glial scars, and inflammation: Inhibitory extracellular matrices and regeneration failure. Exp Neurol. 2008; 209:294–301. [PubMed: 17617407]
25. Franklin SL, Love S, Greene JR, Betmouni S. Loss of perineuronal net in ME7 prion disease. J Neuropathol Exp Neurol. 2008; 67:189–199. [PubMed: 18344910]
26. Freund TF, Buzsaki G. Interneurons of the hippocampus. Hippocampus. 1996; 6:347–470. [PubMed: 8915675]
27. Frischknecht R, Heine M, Perrais D, Seidenbecher CI, Choquet D, Gundelfinger ED. Brain extracellular matrix affects AMPA receptor lateral mobility and short-term synaptic plasticity. Nat Neurosci. 2009; 12:897–904. [PubMed: 19483686]
28. Giamanco KA, Morawski M, Matthews RT. Perineuronal net formation and structure in aggrecan knockout mice. Neuroscience. 2010; 170:1314–1327. [PubMed: 20732394]
29. Hartig W, Brauer K, Bigl V, Bruckner G. Chondroitin sulfate proteoglycan-immunoreactivity of lectin-labeled perineuronal nets around parvalbumin-containing neurons. Brain Res. 1994; 635:307–311. [PubMed: 8173967]
30. Hartig W, Derouiche A, Welt K, Brauer K, Grosche J, Mader M, Reichenbach A, Bruckner G. Cortical neurons immunoreactive for the potassium channel Kv3.1b subunit are predominantly surrounded by perineuronal nets presumed as a buffering system for cations. Brain Res. 1999; 842:15–29. [PubMed: 10526091]
31. Hockfield S, McKay RD. A surface antigen expressed by a subset of neurons in the vertebrate central nervous system. Proc Natl Acad Sci USA. 1983; 80:5758–5761. [PubMed: 6193523]
32. Ida M, Shuo T, Hirano K, Tokita Y, Nakanishi K, Matsui F, Aono S, Fujita H, Fujiwara Y, Kaji T, Oohira A. Identification and functions of chondroitin sulfate in the milieu of neural stem cells. J Biol Chem. 2006; 281:5982–5991. [PubMed: 16373347]
33. Jankowsky JL, Slunt HH, Gonzales V, Jenkins NA, Copeland NG, Borchelt DR. APP processing and amyloid deposition in mice haplo-insufficient for presenilin 1. Neurobiol Aging. 2004; 25:885–892. [PubMed: 15212842]
34. Jaworski DM, Kelly GM, Hockfield S. The CNS-specific hyaluronan-binding protein BEHAB is expressed in ventricular zones coincident with gliogenesis. J Neurosci. 1995; 15:1352–1362. [PubMed: 7869103]
35. Jenkins HG, Bachelard HS. Glycosaminoglycans in cortical autopsy samples from Alzheimer brain. J Neurochem. 1988; 51:1641–1645. [PubMed: 3139840]
36. Kaas JH, Qi HX, Burish MJ, Gharbawie OA, Onifer SM, Massey JM. Cortical and subcortical plasticity in the brains of humans, primates, and rats after damage to sensory afferents in the dorsal columns of the spinal cord. Exp Neurol. 2008; 209:407–416. [PubMed: 17692844]

37. Katsumaru H, Kosaka T, Heizmann CW, Hama K. Immunocytochemical study of GABAergic neurons containing the calcium-binding protein parvalbumin in the rat hippocampus. Exp Brain Res. 1988; 72:347–362. [PubMed: 3066634]
38. Kobayashi K, Emson PC, Mountjoy CQ. *Vicia villosa* lectin-positive neurones in human cerebral cortex. Loss in Alzheimer-type dementia. Brain Res. 1989; 498:170–174. [PubMed: 2790470]
39. Kocherhans S, Madhusudan A, Doehner J, Breu KS, Nitsch RM, Fritschy JM, Knuesel I. Reduced Reelin expression accelerates amyloid-beta plaque formation and tau pathology in transgenic Alzheimer's disease mice. J Neurosci. 2010; 30:9228–9240. [PubMed: 20610758]
40. Koyama R, Yamada MK, Fujisawa S, Katoh-Semba R, Matsuki N, Ikegaya Y. Brain-derived neurotrophic factor induces hyperexcitable reentrant circuits in the dentate gyrus. J Neurosci. 2004; 24:7215–7224. [PubMed: 15317847]
41. Kurazono S, Okamoto M, Sakiyama J, Mori S, Nakata Y, Fukuoka J, Amano S, Oohira A, Matsui H. Expression of brain specific chondroitin sulfate proteoglycans, neurocan and phosphacan, in the developing and adult hippocampus of Ihara's epileptic rats. Brain Res. 2001; 898:36–48. [PubMed: 11292447]
42. Kusakabe M, Mangiarini L, Laywell ED, Bates GP, Yoshiki A, Hiraiwa N, Inoue J, Steindler DA. Loss of cortical and thalamic neuronal tenascin-C expression in a transgenic mouse expressing exon 1 of the human Huntington disease gene. J Comp Neurol. 2001; 430:485–500. [PubMed: 11169482]
43. Lander C, Zhang H, Hockfield S. Neurons produce a neuronal cell surface-associated chondroitin sulfate proteoglycan. J Neurosci. 1998; 18:174–183. [PubMed: 9412498]
44. Lendvai D, Morawski M, Bruckner G, Negyessy L, Baksa G, Glasz T, Patonay L, Matthews RT, Arendt T, Alpar A. Perisynaptic aggrecan-based extracellular matrix coats in the human lateral geniculate body devoid of perineuronal nets. J Neurosci Res. 2012; 90:376–387. [PubMed: 21959900]
45. Matthews RT, Gary SC, Zerillo C, Pratta M, Solomon K, Arner EC, Hockfield S. Brain-enriched hyaluronan binding (BEHAB)/brevican cleavage in a glioma cell line is mediated by a disintegrin and metalloproteinase with thrombospondin motifs (ADAMTS) family member. J Biol Chem. 2000; 275:22695–22703. [PubMed: 10801887]
46. Matthews RT, Kelly GM, Zerillo CA, Gray G, Tiemeyer M, Hockfield S. Aggrecan glycoforms contribute to the molecular heterogeneity of perineuronal nets. J Neurosci. 2002; 22:7536–7547. [PubMed: 12196577]
47. McEwen BS. Stress and hippocampal plasticity. Annu Rev Neurosci. 1999; 22:105–122. [PubMed: 10202533]
48. McGuire PK, Hockfield S, Goldman-Rakic PS. Distribution of cat-301 immunoreactivity in the frontal and parietal lobes of the macaque monkey. J Comp Neurol. 1989; 288:280–296. [PubMed: 2677066]
49. McIntire SL, Reimer RJ, Schuske K, Edwards RH, Jorgensen EM. Identification and characterization of the vesicular GABA transporter. Nature. 1997; 389:870–876. [PubMed: 9349821]
50. McRae PA, Baranov E, Sarode S, Brooks-Kayal AR, Porter BE. Aggrecan expression, a component of the inhibitory interneuron perineuronal net, is altered following an early-life seizure. Neurobiol Dis. 2010; 39:439–448. [PubMed: 20493259]
51. Morawski M, Alpar A, Bruckner G, Fiedler A, Jager C, Gati G, Stieler JT, Arendt T. Chondroitin sulfate proteoglycan-based extracellular matrix in chicken (*Gallus domesticus*) brain. Brain Res. 2009; 1275:10–23. [PubMed: 19269276]
52. Morawski M, Bruckner G, Arendt T, Matthews RT. Aggrecan: beyond cartilage and into the brain. Int J Biochem Cell Biol. 2012; 44:690–693. [PubMed: 22297263]
53. Morawski M, Bruckner G, Jager C, Seeger G, Arendt T. Neurons associated with aggrecan-based perineuronal nets are protected against tau pathology in subcortical regions in Alzheimer's disease. Neuroscience. 2010; 169:1347–1363. [PubMed: 20497908]
54. Morawski M, Bruckner G, Jager C, Seeger G, Matthews R, Arendt T. Involvement of perineuronal and perisynaptic extracellular matrix in Alzheimer's disease neuropathology. Brain Pathol. 2012; 22:547–561. [PubMed: 22126211]

55. Morawski M, Bruckner MK, Riederer P, Bruckner G, Arendt T. Perineuronal nets potentially protect against oxidative stress. Exp Neurol. 2004; 188:309–315. [PubMed: 15246831]
56. Morawski M, Pavlica S, Seeger G, Grosche J, Kouznetsova E, Schliebs R, Bruckner G, Arendt T. Perineuronal nets are largely unaffected in Alzheimer model Tg2576 mice. Neurobiol Aging. 2010; 31:1254–1256. [PubMed: 18829133]
57. Mulder J, Zilberter M, Pasquare SJ, Alpar A, Schulte G, Ferreira SG, Kofalvi A, Martin-Moreno AM, Keimpema E, Tanila H, Watanabe M, et al. Molecular reorganization of endocannabinoid signalling in Alzheimer's disease. Brain. 2011; 134:1041–1060. [PubMed: 21459826]
58. O'Callaghan P, Sandwall E, Li JP, Yu H, Ravid R, Guan ZZ, van Kuppevelt TH, Nilsson LN, Ingelsson M, Hyman BT, Kalimo H, et al. Heparan sulfate accumulation with Abeta deposits in Alzheimer's disease and Tg2576 mice is contributed by glial cells. Brain Pathol. 2008; 18:548–561. [PubMed: 18422760]
59. Ojima H, Sakai M, Ohyama J. Molecular heterogeneity of *Vicia villosa*-recognized perineuronal nets surrounding pyramidal and nonpyramidal neurons in the guinea pig cerebral cortex. Brain Res. 1998; 786:274–280. [PubMed: 9555057]
60. Palop JJ, Mucke L. Epilepsy and cognitive impairments in Alzheimer disease. Arch Neurol. 2009; 66:435–440. [PubMed: 19204149]
61. Pavlov I, Rauvala H, Taira T. Enhanced hippocampal GABAergic inhibition in mice overexpressing heparin-binding growth-associated molecule. Neuroscience. 2006; 139:505–511. [PubMed: 16473473]
62. Perosa SR, Porcionatto MA, Cukiert A, Martins JR, Amado D, Nader HB, Cavalheiro EA, Leite JP, Naffah-Mazzacoratti MG. Extracellular matrix components are altered in the hippocampus, cortex, and cerebrospinal fluid of patients with mesial temporal lobe epilepsy. Epilepsia. 2002; 43(Suppl 5):159–161. [PubMed: 12121313]
63. Perosa SR, Porcionatto MA, Cukiert A, Martins JR, Passeroti CC, Amado D, Matas SL, Nader HB, Cavalheiro EA, Leite JP, Naffah-Mazzacoratti MG. Glycosaminoglycan levels and proteoglycan expression are altered in the hippocampus of patients with mesial temporal lobe epilepsy. Brain Res Bull. 2002; 58:509–516. [PubMed: 12242104]
64. Pizzorusso T, Medini P, Berardi N, Chierzi S, Fawcett JW, Maffei L. Reactivation of ocular dominance plasticity in the adult visual cortex. Science. 2002; 298:1248–1251. [PubMed: 12424383]
65. Schnell SA, Staines WA, Wessendorf MW. Reduction of lipofuscin-like autofluorescence in fluorescently labeled tissue. J Histochem Cytochem. 1999; 47:719–730. [PubMed: 10330448]
66. Schuppel K, Brauer K, Hartig W, Grosche J, Earley B, Leonard BE, Bruckner G. Perineuronal nets of extracellular matrix around hippocampal interneurons resist destruction by activated microglia in trimethyltin-treated rats. Brain Res. 2002; 958:448–453. [PubMed: 12470883]
67. Suzuki K, Katzman R, Korey SR. Chemical studies on Alzheimer's disease. J Neuropathol Exp Neurol. 1965; 24:211–224. [PubMed: 14280498]
68. Vidal E, Bolea R, Tortosa R, Costa C, Domenech A, Monleon E, Vargas A, Badiola JJ, Pumarola M. Assessment of calcium-binding proteins (parvalbumin and calbindin D-28K) and perineuronal nets in normal and scrapie-affected adult sheep brains. J Virol Methods. 2006; 136:137–146. [PubMed: 16828173]
69. Watanabe H, Kimata K, Line S, Strong D, Gao LY, Kozak CA, Yamada Y. Mouse cartilage matrix deficiency (cmd) caused by a 7 bp deletion in the aggrecan gene. Nat Genet. 1994; 7:154–157. [PubMed: 7920633]
70. Wegner F, Hartig W, Bringmann A, Grosche J, Wohlfarth K, Zuschratter W, Bruckner G. Diffuse perineuronal nets and modified pyramidal cells immunoreactive for glutamate and the GABA(A) receptor alpha1 subunit form a unique entity in rat cerebral cortex. Exp Neurol. 2003; 184:705–714. [PubMed: 14769362]
71. Wu Y, Wu J, Lee DY, Yee A, Cao L, Zhang Y, Kiani C, Yang BB. Versican protects cells from oxidative stress-induced apoptosis. Matrix Biol. 2005; 24:3–13. [PubMed: 15748997]
72. Yamada H, Fredette B, Shitara K, Hagihara K, Miura R, Ranscht B, Stallcup WB, Yamaguchi Y. The brain chondroitin sulfate proteoglycan brevican associates with astrocytes ensheathing

cerebellar glomeruli and inhibits neurite outgrowth from granule neurons. J Neurosci. 1997; 17:7784–7795. [PubMed: 9315899]

73. Yamaguchi Y. Lecticans: organizers of the brain extra-cellular matrix. Cell Mol Life Sci. 2000; 57:276–289. [PubMed: 10766023]

Europe PMC Funders Author Manuscripts

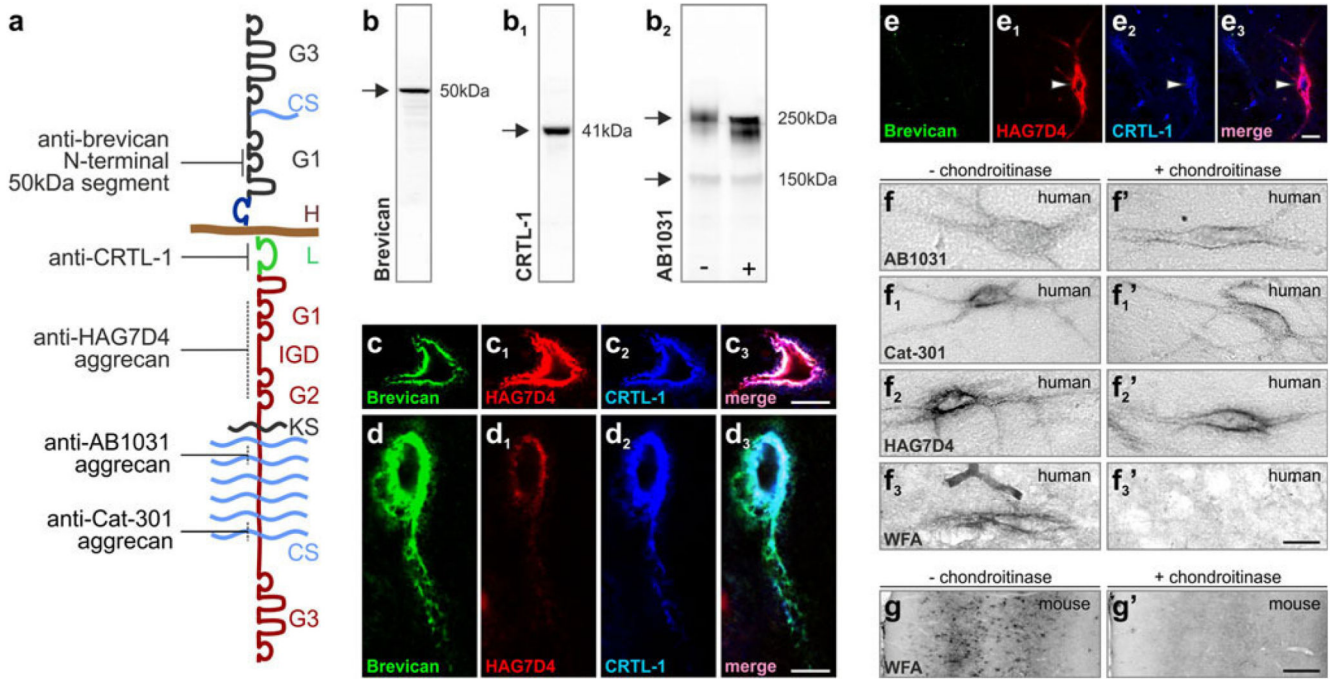

Fig. 1.

Molecular identity and structure of hyaluronan-based extracellular matrix components. **a** Molecular relationship of aggrecan, brevican and hyaluronan (H) forming multi-molecular complexes. *Solid lines* indicate discrete epitopes recognized by the antibodies. *Dashed lines* denote putative antibody recognition sites. **b–b$_2$** Representative Western blots of brevican (**b**), CRTL-1 (**b$_1$**) and aggrecan (AB1031, **b$_2$**) from mouse brain showing a primary protein band at the calculated molecular weight of each target. **b$_2$** Chondroitinase ABC-induced gel-shift of the >250 kDa, slow-migrating isoforms of aggrecan (AB1031) was used to validate their recognition by the AB1031 antibody. **c–e$_3$** Co-localization of major extracellular matrix components around hippocampal neurons. **c–c$_3$** Perineuronal nets commonly contained aggrecan (HAG7D4) and cartilage-related “link” protein 1 (CTRL-1; *arrowhead*) but not brevican. **d–e$_3$** Examples of brevican (50 kDa)$^+$/aggrecan (HAG7D4$^+$)/CRTL-1$^+$ perineuronal nets of the conventional type [70]. **f–f$_3$′** In human *post-mortem* hippocampus, chondroitinase digestion did not alter appearance of aggrecan$^+$ perineuronal nets but completely abolished occasional WFA lectin labelling (**f$_3$–f$_3$′**). **g**, **g′** The lack of WFA labelling confirmed the efficacy of chondroitinase treatment in simultaneously processed sections from mouse brain. *CS* chondroitin sulphate chains, *G1/G2* N-terminal globular domains, *G3* C-terminal globular domain, *IGD* interglobular domain, *KS* keratin sulphate chains, *L* CRTL-1. *Scale bars* 100 μm (**g**, **g′**), 10 μm (**c$_3$**, **e$_3$**, **f–f$_3$′**), 5 μm (**d$_3$**)

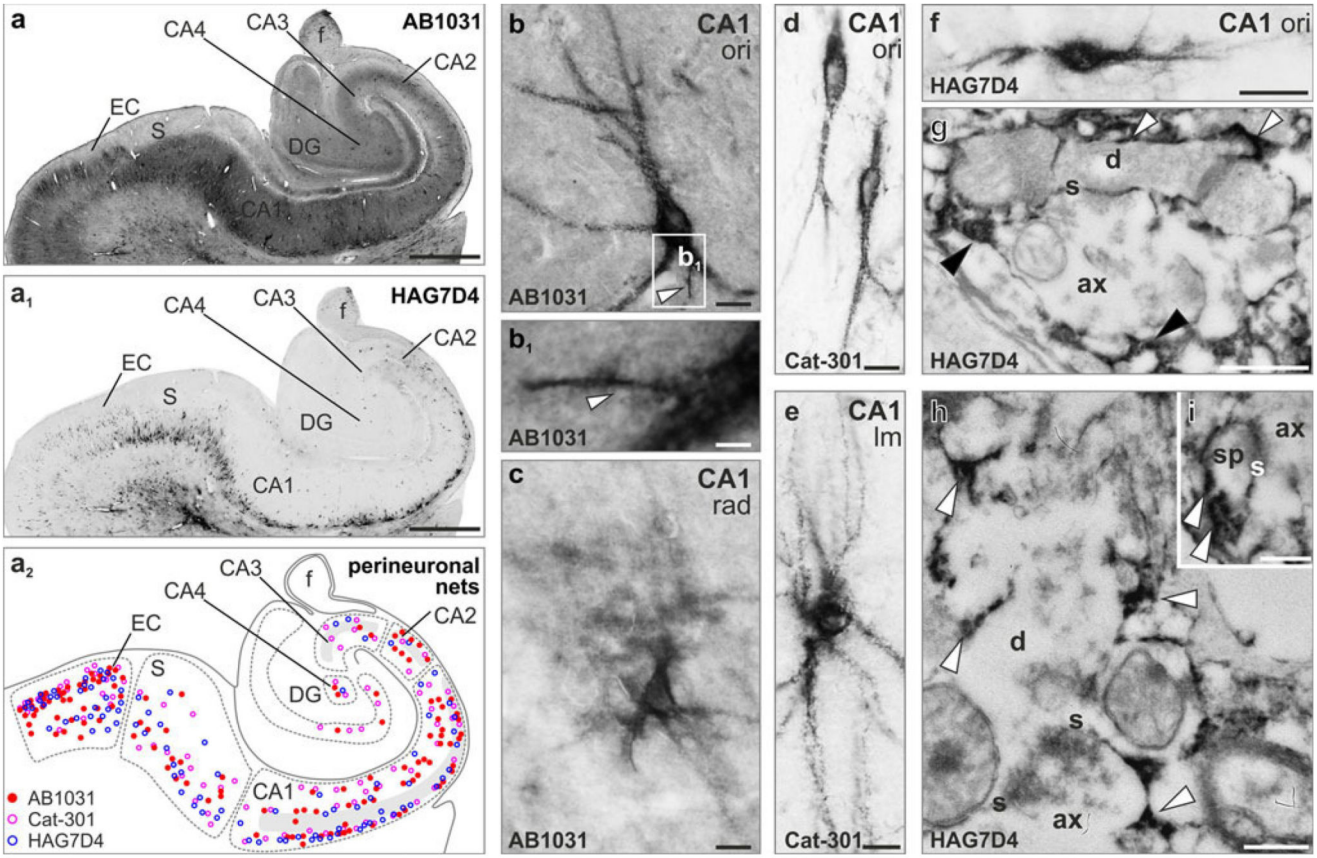

Fig. 2.

Distribution of aggrecan-containing perineuronal nets in the human hippocampus (**a–a$_2$**). Distribution of AB1031$^+$ (**a**, *solid red circles* in **a$_2$**), Cat-301$^+$ (*open pink circles* in **a$_2$**) and HAG7D4$^+$ (**a$_1$**, *open blue circles* in **a$_2$**) perineuronal nets in identified hippocampal subfields and the entorhinal cortex (EC). *Grey shading* in **a$_2$** labels the CA1-CA3 pyramidal layer. **b–c** Phenotypic appearance of AB1031$^+$ perineuronal nets. Both “classical” sharp-contoured (**b**) and diffuse perineuronal nets (**c**) were identified throughout the hippocampal formation. Axon initial segments (*arrowheads* in **b**, **b$_1$**) were visualized in several cases. **d, e** Cat-301$^+$ perineuronal nets were typically of granular appearance and surrounded first, second or higher order dendrites. **f** HAG7D4$^+$ perineuronal matrices in the CA1 stratum oriens (ori). **g, h** Ultrastructural analysis showed that HAG7D4$^+$ aggrecan matrix (*arrowheads*) surrounded axons, but most particularly dendritic profiles in CA1. **i** Axo-spiny synapse embedded in HAG7D4$^+$ extracellular matrix (*arrowheads*). For detailed description of region- and layer-specific distribution and phenotypes of aggrecan$^+$ perineuronal nets see Fig. S1-3. The supplementary list of abbreviations contains description of all anatomical structures. *Scale bars* 500 μm (**a–a$_1$**), 10 μm (**b–f**), 4 μm (**b$_1$**), 500 nm (**g**), 250 nm (**h, i**)

Europe PMC Funders Author Manuscripts

Europe PMC Funders Author Manuscripts

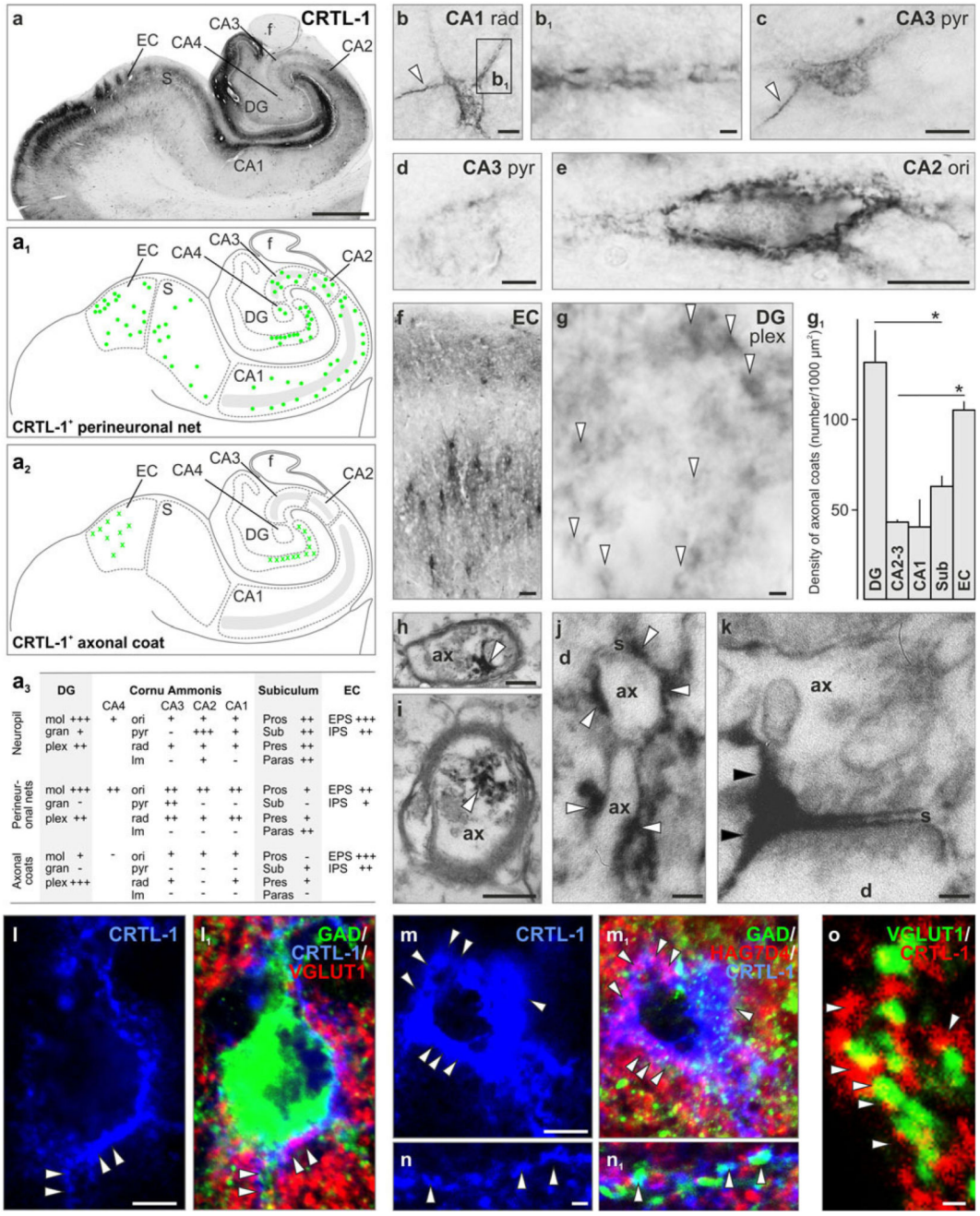

a3

	DG	Cornu Ammonis				Subiculum		EC
		CA4		CA3	CA2	CA1			
Neuropil	mol +++	+	ori	+	+	+	Pros ++	EPS +++
	gran +		pyr	-	+++	+	Sub ++	IPS ++
	plex ++		rad	+	+	+	Pres ++	
			lm	-	+	-	Paras ++	
Perineuronal nets	mol +++	++	ori	++	++	++	Pros +	EPS ++
	gran -		pyr	++	-	-	Sub -	IPS +
	plex ++		rad	++	+	++	Pres +	
			lm	-	-	-	Paras ++	
Axonal coats	mol +	-	ori	+	+	+	Pros -	EPS +++
	gran -		pyr	-	-	-	Sub +	IPS ++
	plex +++		rad	+	-	+	Pres +	
			lm	-	-	-	Paras -	

Fig. 3.

Perineuronal nets and axonal coats contain cartilage link protein 1 (CRTL-1). **a–a$_2$** CRTL-1 distribution in the human hippocampus. Note that besides its more conventional perineuronal net localization in non-pyramidal layers (**a$_1$**), CRTL-1$^+$ axonal coats (**a$_2$**) were seen in the dentate gyrus (DG) and entorhinal cortex (EC). *Grey shading* labels the CA1-CA3 pyramidal layer. **a$_3$** Semi-quantitative analysis of CRTL-1 distribution and density (– not present, +/++/+++ low/moderate/high frequency) in the DG, cornu ammonis (CA) subfields, subiculum and entorhinal cortex (EC). **b, c** Perineuronal nets in CA1 stratum radiatum (rad)

and CA3 stratum pyramidale (pyr) frequently outlined axon initial segment (*arrowheads*). **b_1** Peridendritic sheath. **d** Matrix assembly restricted to the perisomatic region of a neuron in CA3 stratum pyramidale (pyr). **e** Perisomatic and proximal dendritic labelling in CA2 stratum oriens (ori). **f** Perineuronal nets at considerable density in the EC's external and internal principal strata (EPS/IPS). **g** Axonal coats (*open arrowheads*) at the hilar border of the DG. **g_1** The density of axonal coats was highest in the DG and EC. **h, i** CRTL-1 in mylinated axons. **j, k** CRTL-1^+ matrix concentrates around terminal axon segments (*open arrowheads*) or selectively around synapses (*solid arrowheads*). **l–m_1** GAD^+ and $VGLUT1^+$ profiles (*arrowheads*) embedded in the classical (**l, l_1**) or diffuse (**m, m_1**) type of CRTL-1^+ perineuronal matrix [70]. **n, n_1** $HAG7D4^+$/CRTL-1^+ peridendritic sheaths enwrap $GAD65/67^+$ terminals (*arrowheads*). **o** CRTL-1^+ axonal coats engulf $VGLUT1^+$ excitatory synapses. Refer the supplementary list of abbreviations for designation of particular anatomical structures. **g_1** Data were expressed as mean ± SEM, $*p < 0.05$. *Scale bars* 500 μm (**a**), 20 μm (**f**), 10 μm (**b, c, l–l_1, m–m_1**), 5 μm (**d, e**), 2 μm (**b_1, g, n–n_1, o**), 250 nm (**i**), 100 nm (**h, j, k**)

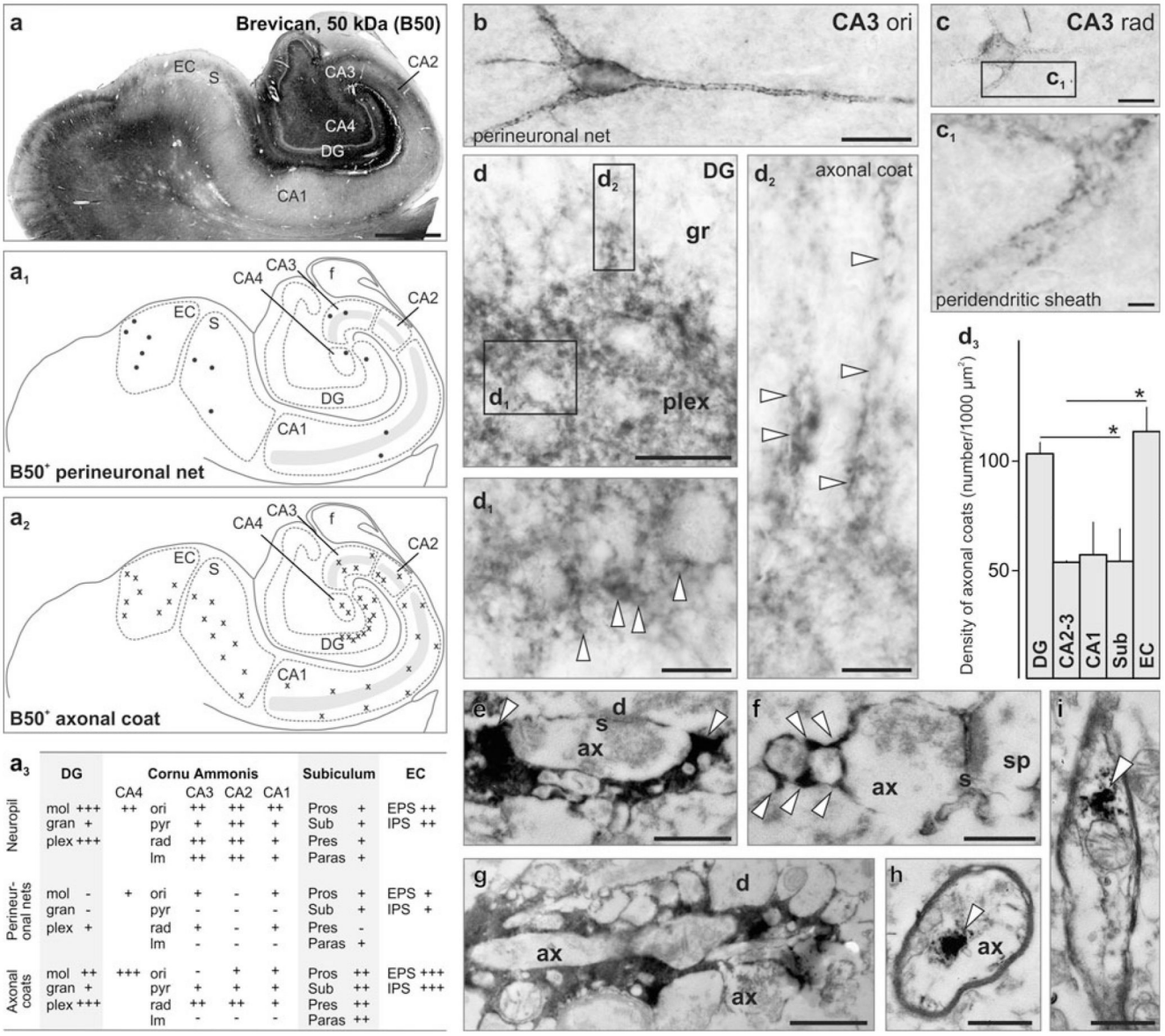

a3

	DG		Cornu Ammonis				Subiculum		EC
		CA4		CA3	CA2	CA1			
Neuropil	mol +++	++	ori	++	++	++	Pros	+	EPS ++
	gran +		pyr	+	++	+	Sub	+	IPS ++
	plex +++		rad	++	++	+	Pres	+	
			lm	++	++	+	Paras	+	
Perineuronal nets	mol -	+	ori	+	-	+	Pros	+	EPS +
	gran -		pyr	-	-	-	Sub	+	IPS +
	plex +		rad	+	-	+	Pres	-	
			lm	-	-	-	Paras	+	
Axonal coats	mol ++	+++	ori	-	+	+	Pros	++	EPS +++
	gran +		pyr	+	+	+	Sub	++	IPS +++
	plex +++		rad	++	++	+	Pres	++	
			lm	-	-	-	Paras	++	

Fig. 4.

Brevican preferentially labels axonal coats in the human hippocampus. **a** Overview of brevican immunoreactivity in the human hippocampal formation. Schema of the distribution of perineuronal nets (**a$_1$**) and axonal coats (**a$_2$**). *Grey shading* marks the CA1–CA3 pyramidal layer. **a$_3$** Semi-quantitative analysis of Brevican distribution and density (− not present, +/++/+++ low/moderate/high frequency) in the DG, cornu ammonis (CA) subfields, subiculum and entorhinal cortex (EC). **b, c** Examples of perineuronal nets in strata oriens (ori; **b**) and radiatum (rad; c) of the CA3 subfield. *Inset* (**c$_1$**) shows peridendritic sheath. **d–d$_2$** Axonal coats (*arrowheads*) at the DG hilar border. **d$_2$** Chains of axonal coats occasionally invaded the dense granule cell layers. **d$_3$** The density of axonal coats was highest in dentate gyrus and entorhinal cortex. **e–g** Brevican$^+$ axonal coats typically enwrapped the presynaptic compartment of synapses (*arrowheads*). **h, i** Brevican intracellularly in axons. **d$_3$** Regional

density of axonal coats in the human hippocampus. Data were expressed as mean ± SEM, *$p < 0.05$. The supplementary list of abbreviations contains designation of particular subcellular compartments and brain regions. *Scale bars* 500 μm (**a**), 10 μm (**b, c**), 5 μm (**d**), 4 μm (**c, d_1, d_2**), 500 nm (**i**), 250 nm (**e–h**)

Europe PMC Funders Author Manuscripts

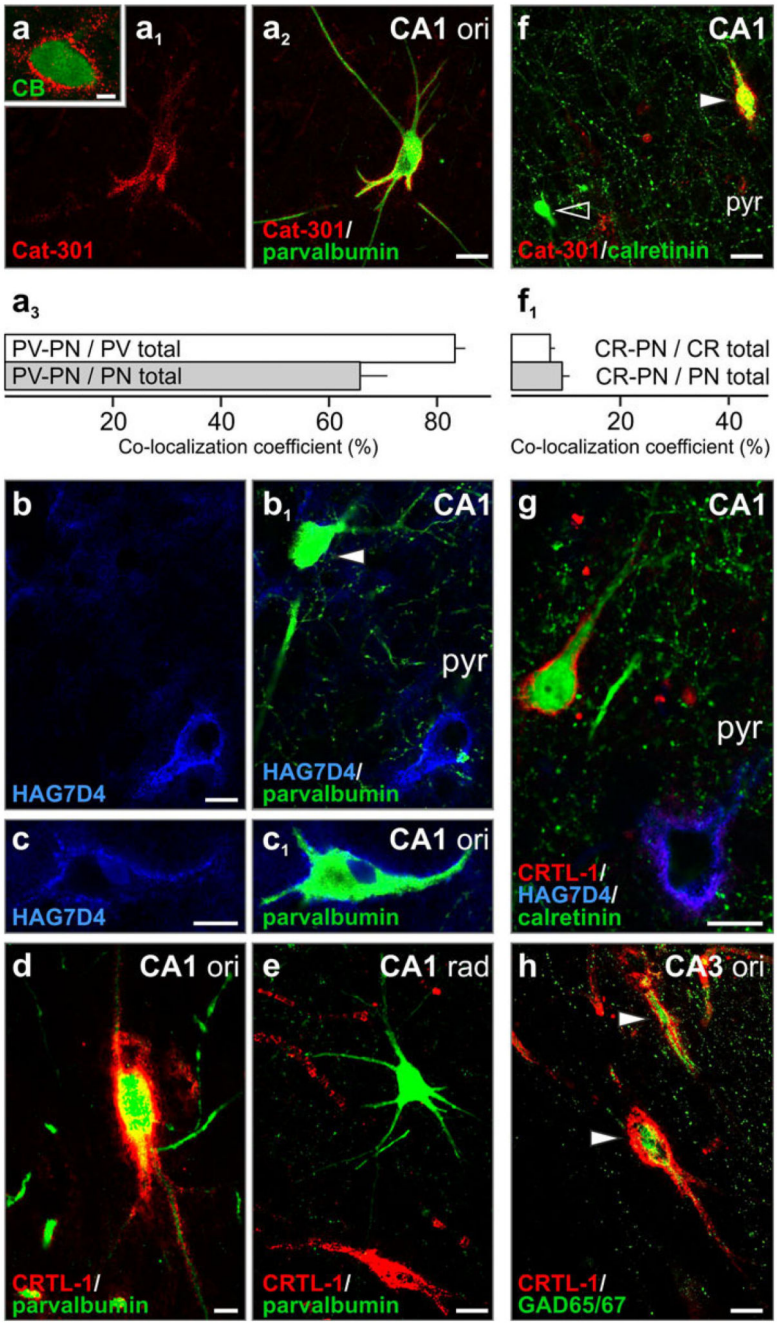

Fig. 5.

Perineuronal nets co-localize with all Ca^{2+}-binding proteins. **a** Aggrecan co-localizes with calbindin D28k (CB) in the CA4. **a_1–c_1** Aggrecan-containing perineuronal nets around parvalbumin$^+$ neurons. *Arrowhead* denotes a parvalbumin$^+$ interneuron devoid of perineuronal net. **a_3** The majority (83 %) of all parvalbumin$^+$ neurons (PV total) were found surrounded by Cat-301$^+$ perineuronal nets (PV-PN) whilst 66 % of all perineuronal net-bearing neurons (PN total) showed parvalbumin immunoreactivity (PV-PN). **d, e** CRTL-1$^+$ perineuronal nets enwrap parvalbumin$^+$ neurons in the stratum oriens (ori; **d**) but not in

stratum radiatum (rad; **e**). **f** Perineuronal nets surround calretinin$^+$ neurons (*solid arrowhead*). *Open arrowhead* points to a calretinin$^+$ neuron. **f$_1$** The proportion of perineuronal net-bearing calretinin$^+$ neurons (CR-PN) was low (7 % amongst all calretinin$^+$ cells, and 9 % for all net-bearing neurons). **g** CRTL-1$^+$/HAG7D4− perineuronal net surrounds calretinin$^+$ CA1 neuron. **h** GAD65/67$^+$ somata and processes were invariably encapsulated by CRTL-1$^+$ perineuronal matrix (*arrowheads*). Quantitative data were expressed as mean ± SEM. *Scale bars* 10 μm (**a$_1$–h**), 2 μm (**a**)

Europe PMC Funders Author Manuscripts

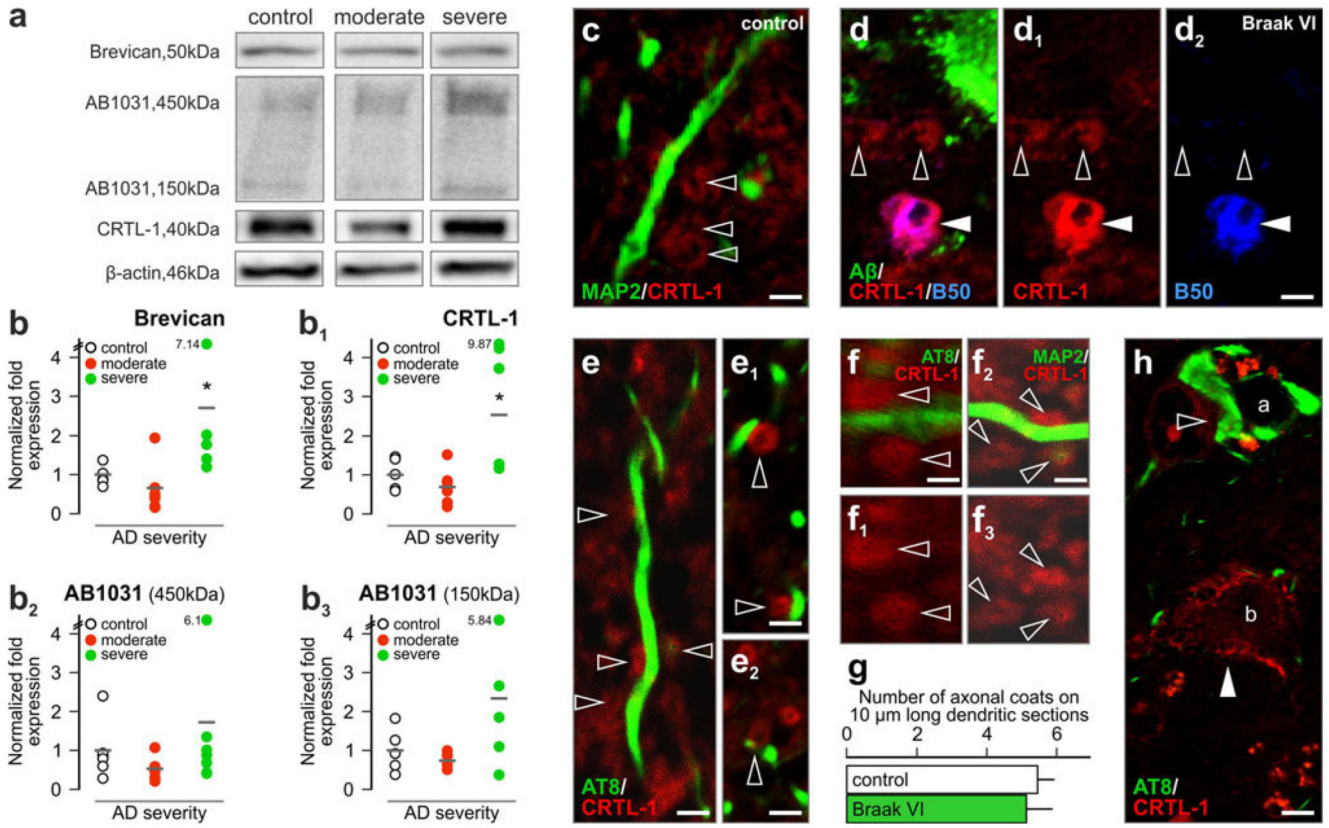

Fig. 6.

Extracellular matrix components in Alzheimer's disease. **a** Western blot detection of brevican, aggrecan (AB1031) and CRTL-1 in control and moderate/severe Alzheimer's disease subjects (representative images). Sample cohorts were run simultaneously on the same gel, and analysed *off*-line. **b–b$_3$** Severe AD subjects show marked increases in all investigated matrix proteins. Note the large individual variations in the Braak VI ("severe") group. **c** Axonal coats (*open arrowheads*) in the dentate gyrus of the human hippocampus. **d–d$_2$** Axonal coats proximal to senile plaques. *Solid* and *open arrowheads* indicate dual- and single-labelled axonal coat, respectively. **e–e$_2$** CRTL-1$^+$ axonal coats apposing tau-containing dendrites. **f–g** Quantitative analysis of axonal coat density along identified dendrite segments. AT8 (AD) and MAP2 (control) were used to dissociate dendrites with/without cytoskeletal pathology. **h** AT8-immunoreactive (*open arrowhead*) soma (**a**) lacking a perineuronal net but targeted by afferents surrounded with axonal coats. Perineuronal net (*solid arrowhead*) surrounded tau$^-$ neurons (**b**). **g** Data were expressed as mean ± SEM, $p < 0.05$. *Scale bars* 2 µm (**c–d$_2$, h**), 1.5 µm (**e–f$_2$**)

Europe PMC Funders Author Manuscripts

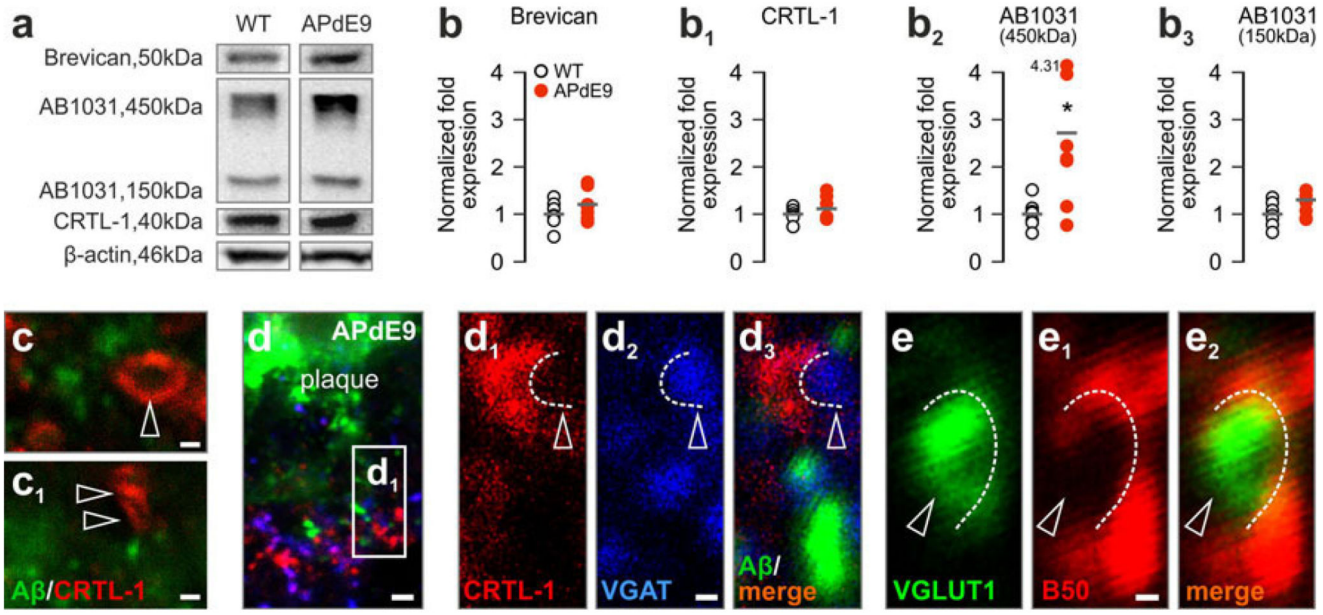

Fig. 7.

Extracellular matrix assembly in APdE9 transgenic mice. **a** Representative blot images of brevican, aggrecan (AB1031) and CRTL-1 from 10-month-old wild-type (WT) and APdE9 transgenic mice. **b–b_3** Levels of CSPG matrix components in APdE9 versus WT mice. **c, c_1, d** Axonal coats (*arrowheads*) are present in the immediate proximity of Aβ deposits in APdE9 mice and surround $VGAT^+$ (**d_1–d_3**) or $VGLUT1^+$ (**e–e_2**) synaptic profiles (*open arrowheads*). *Scale bars* 2 μm (**d**), 1 μm (**c, c_1, d_2, e_1**)

Europe PMC Funders Author Manuscripts